



ELSEVIER

Nuclear Instruments and Methods in Physics Research A 414 (1998) 332–339

**NUCLEAR
INSTRUMENTS
& METHODS
IN PHYSICS
RESEARCH**
Section A

Diffusely reflective aerogel Cherenkov detector simulation techniques

D.W. Higinbotham

Department of Physics, University of Virginia, Charlottesville, VA 22901, USA

Received 19 March 1996; received in revised form 5 May 1998

Abstract

Due to the similarity of construction materials used in large diffusely reflective aerogel Cherenkov detectors, a reasonable prediction of a detector's photoelectron signal can be made using a phenomenological equation and parameters easily determined prior to construction. By using the same parameters and Monte Carlo techniques, it is possible not only to predict the photoelectron signal; but also, the uniformity of the signal, the average number of photomultiplier tubes which trigger per event, and the timing resolution of the detector. In this paper both techniques are described and it is shown that even though they use only a minimal number of parameters, both reproduce experimental results and can be used to quickly model detector designs. © 1998 Elsevier Science B.V. All rights reserved.

1. Introduction

The most important consideration when designing a large, diffusely reflective aerogel Cherenkov detector is how many photoelectrons will be detected per relativistic event. This photoelectron signal, typically less than ten photoelectrons, determines the detector's efficiency for detecting relativistic particles. Many calculational techniques have been used to predict this signal [1–3]; however, the techniques all require designers to estimate some details of a detector's construction, such as the average reflectivity of the light box region of the detector, the absolute efficiency of the photomultiplier tubes, and the number of photons entering the light box. Though these estimates are fine for making an order of magnitude calculation, they are not a reliable method of making accurate predictions of

a detector's photoelectron signal, nor do they give any indication of the uniformity of the signal.

Without a reliable method of predicting the photoelectron signal or the uniformity of the signal, designers cannot reliably determine either how much aerogel or how many photomultipliers a detector will need to produce a sufficient and uniform photoelectron signal. This has meant that designers have often overestimated how much aerogel and/or how many photomultiplier tubes a detector would need. Since the photomultiplier tubes and related electronics tend to be the most expensive components of an aerogel Cherenkov detector, using only the required number can greatly reduce detector construction costs.

Previous work has shown that a figure of merit curve, calculated from experimental results, can be used to reduce the number of parameters that are

needed to calculate the photoelectron signal [4]. This is done by including in a figure of merit several parameters that cannot be measured until after construction. The present work takes this idea one step further by including in a figure of merit all parameters which cannot be determined prior to construction. This results in a phenomenological equation, derived in Section 2, in which the photoelectron signals from previous Cherenkov detector results are used to calculate a figure of merit. These results, shown in Sections 4 and 5, can then in turn be used to estimate the number of photoelectrons a detector will produce.

Though the phenomenological equation can provide a good estimate of the photoelectron signal, no information about signal uniformity, timing, or the multiplicity – the average number of photomultiplier tubes which trigger per event – is produced. In order to provide this information, a Monte Carlo program, which also uses only parameters easily determined prior to construction, has been developed and is described in Section 3.

In Section 4, the phenomenological equation and the Monte Carlo program are used to calculate the figure of merit for numerous existing large

Cherenkov detectors. These results are summarized in Table 1 and are presented in Fig. 5. The numerous results shown in the figure are intended not only to provide designers with the figure of merit but also to give an impression of the variation in results that have been obtained by previous groups.

In Section 5 the usage of the new, long attenuation length aerogel is considered. It is shown that the simulation code only needs to be modified slightly to account for the new aerogel and a new figure of merit is derived for the phenomenological equation. Finally, in Section 6 the average lifetime of an aerogel Cherenkov detector is discussed.

2. Phenomenological simulation equation

In a diffusely reflective aerogel Cherenkov detector, radiation is produced in layers of highly porous aerogel. Photons of a given frequency are emitted in the aerogel when the speed of a charged particle passing through the material is greater than the phase velocity of the associated electromagnetic fields of the same frequency [5]. This

Table 1

Shown is a comparison of simulation values versus experimental values for various large diffusely reflective aerogel Cherenkov detectors. Also shown are all of the variable values used in the calculations, where η is the average reflectivity of the light box area, ε the fraction of the light box area covered by photomultiplier tubes, n the refractive index of the aerogel, β the velocity divided by the speed of light, and L the thickness of the aerogel

Light box dimensions (cm ³)	η (%)	ε (%)	n	β	L (cm)	Sim. N_e	Exp. N_e	Sim. H (cm ⁻¹)	Exp. H (cm ⁻¹)	Ref.
40 × 140 × 31	92	2.6	1.06	0.981	9.0	4.3	4.1 ^a	26	25	[11]
105 × 50 × 15	90	4.0	1.05	1	9.0	7.2	6.8	29	27	—
132 × 14 × 11	91	9.6	1.05	1	12.5	15	17	24	27	[20]
132 × 14 × 11	91	9.6	1.05	1	12.5	15	13	24	21	[10]
100 × 40 × 15	90	13	1.04	1	9.0	11	5.5	28	14	[9]
100 × 40 × 15	90	13	1.04	1	9.0	11	20	28	51	[9]
40 × 80 × 30 ^b	92	3.7	1.03	0.998	18	5.9	5.5 ^a	18	17	[21]
30 × 69 × 30 ^b	93	5.0	1.03	0.998	18	7.4	6.0 ^a	18	15	[21]
27 × 28 × 15	92	6.5	1.03	1	9.0	6.3	7.5 ^a	26	31	[22]
18 × 52 × 64.5	95	2.8	1.03	0.995	4.5	2.4	2.9	32	39	[8]
18 × 52 × 60.0	94	3.0	1.03	0.995	9.0	3.9	4.6	26	30	[8]
18 × 52 × 55.5	94	3.2	1.03	0.995	13.5	4.9	5.4	21	23	[8]

^aAverage calculated from uniform curves.

^bApproximated as rectangular with tubes mounted directly to detector.

condition can be expressed by the inequality

$$\beta n(\omega) > 1, \quad (1)$$

where $n(\omega)$ is the refractive index of the material for a frequency ω and β is the velocity of the charged particle divided by the speed of light in vacuum. Over the detection range of a typical detector, the refractive index of aerogel can be considered to have no frequency dependence. Aerogel can be produced with refractive indexes between approximately $n = 1.01$ and $n = 1.20$ [6].

The number of photons produced per interval of wavelength by a relativistic particle passing through aerogel is given by

$$\frac{dN}{d\lambda} = 2\pi\alpha L \left(1 - \frac{1}{\beta^2 n^2}\right) \frac{1}{\lambda^2}, \quad (2)$$

where N is the number of photons, λ is the wavelength of the photons, α is the fine structure constant, and L is the path length of the charged particle through the aerogel. From this equation one can calculate N ,

$$N = \int \frac{dN}{d\lambda} d\lambda = CL \left(1 - \frac{1}{\beta^2 n^2}\right), \quad (3)$$

where C is a constant.

The photons are emitted in a cone with an opening angle,

$$\theta = \cos^{-1} \frac{1}{\beta n}, \quad (4)$$

centered on the charged particle's velocity vector. The simulation techniques used in this paper require that these photons be directed towards the light box region of the detector. This is the region outside the aerogel where the photons are reflected and detected (see Fig. 1).

Due to scattering and absorption of radiation in the aerogel, not all of the photons produced in the aerogel enter the light box region. To calculate the number of photons that enter the light box region, the L term can be replaced with L_{eff} ,

$$L_{\text{eff}} = A_a \left[1 - \exp\left(\frac{-L}{A_a}\right) \right], \quad (5)$$

where L_{eff} is the effective thickness of the aerogel and A_a is the effective absorption length of the aerogel. However, since the effective absorption length varies from one batch of aerogel to another and is difficult to measure, it is subsumed into the figure of merit.

Photons which do pass through the aerogel enter into the light box region of the detector. The walls of this region are covered with a diffusely reflective material and the region is viewed by photomultiplier tubes. For photons in the light box region, the surface of the aerogel can be considered to be a diffusely reflective wall [2,7].

To calculate the probability that an individual photon in the light box area will strike the face of

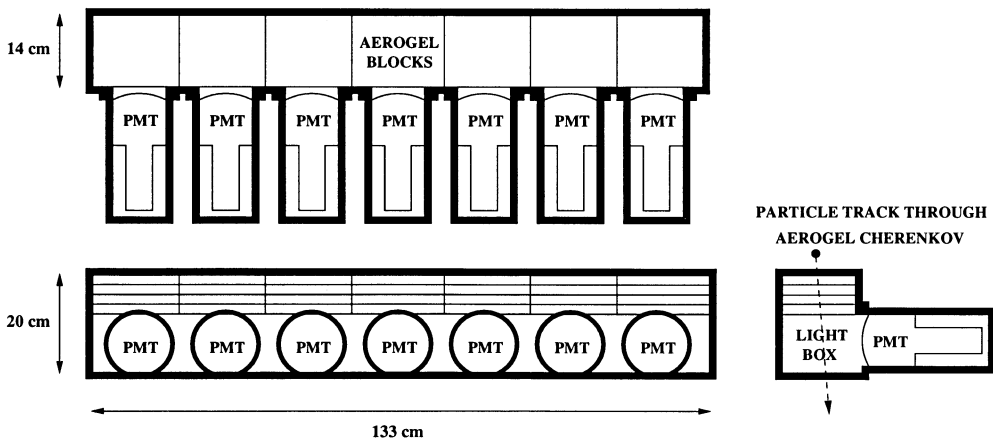


Fig. 1. The schematic diagram shows the NIKHEF EMIN Hall Cherenkov. Shown is the direction of a particle track through an aerogel Cherenkov detector. The Cherenkov light produced in the aerogel is emitted into the diffusely reflective light box region of the detector and is detected by photomultiplier tubes, labeled PMT, located along the walls of the light box.

a photomultiplier, it is assumed that the photon reflections are random. This allows the detection probability to be expressed as a geometric series

$$\sum_{n=0}^{\infty} \varepsilon[\eta(1-\varepsilon)]^n = \frac{\varepsilon}{1-\eta(1-\varepsilon)}, \quad (6)$$

where ε is the fraction of the light box area covered by photomultiplier tubes, η the average reflectivity of the light box area, and $\eta(1-\varepsilon)$ the probability of a photon striking a surface and being reflected. When calculating the average reflectivity of a light box for use with the figure of merit determined in this paper, the diffusely reflective wall should always be taken as having an average reflectivity of 96% [8] and the aerogel as having an average reflectivity of 80% [3].

The phenomenological simulation equation is written by multiplying the number of photons produced (3) by the detection probability (6) by a figure of merit

$$N_e = HL(1 - 1/\beta^2 n^2) \frac{\varepsilon}{1 - \eta(1 - \varepsilon)}, \quad (7)$$

where N_e is the average number of photoelectrons and H the experimentally determined figure of merit. Subsumed in the figure of merit are the constants and the other variables, such as the photomultiplier quantum efficiency, the shape of the light box, and the effective aerogel thickness. However, due to the similarity of materials used in aerogel Cherenkov detectors, the H parameter depends to a good approximation only on the thickness of the aerogel used in the detector. Derived values for the figure of merit are shown in Sections 4 and 5.

The calculated number of photoelectrons, N_e , can be used to estimate the detection efficiency, ξ , of the detector from

$$\xi = 1 - \exp^{-N_e}. \quad (8)$$

Since Eq. (8) assumes Poisson statistics, in order for it to be valid for N_e less than 10 photoelectrons, the photomultiplier tubes need to be able to clearly resolve single photoelectron signals. This resolution allows an average signal of only five photoelectrons to provide 99% detection efficiency.

3. Computer simulation

To complement the phenomenological equation, a computer simulation program was written which also uses only easily determined variables. Unlike the simulation equation, the simulation program takes into account a detector's geometry and the position of the photomultiplier tubes. This allows the program not only to predict the average number of photoelectrons, but also to predict the uniformity, timing resolution, and the photomultiplier multiplicity. This additional information is useful for determining the optimal position and number of photomultiplier tubes and for testing the properties of a three-dimensional design.

The variables used in this simulation are the size of the light box, the refractive index of the aerogel, the number and location of the photomultiplier tubes, the radius of the cathode area of the photomultiplier tubes, the path length of particles through the aerogel, and the β of the particles. All other parameters, such as photomultiplier efficiency and effective absorption length, have been fixed to average values. This is justified by the similarity of materials used in these detectors.

What makes this simulation even more striking is that no attempt is made to simulate the light production in the aerogel. Instead, the Cherenkov light is approximated as originating from the point that the radiating particle exited the aerogel and having a random direction. This approximation, which is also made in the phenomenological equation, is justified by the relatively short scattering length of aerogel compared to the typical thicknesses of aerogel used in diffusely reflective Cherenkov detectors.

An advantage of this approximation¹ is it allows the program to be focused solely on the behavior of light in the light box region of a detector. This reduces the complexity of the program and allows full three-dimensional simulations to be done relatively quickly while still producing results which are in good agreement with actual detectors.

¹ This approximation breaks down if the thickness of aerogel used is less than or equal to the aerogel's scattering length. In this case the Cherenkov angle should be used.

The simulation calculates the average number of photons that are emitted from the aerogel per event, N_{emit} , from the equation

$$N_{\text{emit}} = \int_{\lambda_1}^{\lambda_2} 2\pi\alpha L_{\text{eff}} \left(1 - \frac{1}{\beta^2 n^2}\right) \frac{1}{\lambda^2} d\lambda. \quad (9)$$

Then the program individually tracks that number of photons as they are diffusely reflected about the light box. This process is repeated for thousands of events to produce statistically meaningful results.

Since only well-known variables are entered as input, the other typical variables have been set to the following working values: diffuse wall reflectivity = 96%, aerogel reflectivity = 80%, photomultiplier tube window transmission = 60%, photomultiplier tube detection efficiency = 22%, and absorption length $\lambda_a = 9$ cm. The detected wavelengths are taken to be between 300 and 400 nm. These values do not necessarily correspond to the exact physical values of any one detector but, taken as a group, they produce results that compare very well with average Cherenkov results.

In Table 1, the computer simulated number of photoelectrons, Sim. N_e , for various Cherenkov detectors is shown and compared with the experimental values, Exp. N_e . The only photoelectron value that the simulation program significantly overestimates is the original CEBAF detector result of 5.5 photoelectrons. It was subsequently determined that the aerogel of this detector had become contaminated and needed to be refurbished [9]. After complete refurbishment of the detector and baking of the aerogel, the remarkable value of 20 photoelectrons was obtained, a value consistent with the new aerogels discussed in Section 5. All the detectors listed used Millipore paper as the diffuse reflector and large, high gain photomultiplier tubes such as the Burle 8854 (RCA 8854), the Hamamatsu R1584-01, or the Philips XP2041.

A more detailed comparison between the simulation program and experimental results was made with the recently refurbished NIKHEF QDQ Cherenkov detector [10]. During commissioning, this detector was found to have an average signal of 13 photoelectrons and an average photomultiplier multiplicity of 4. This compares quite well with the simulation, which predicted 15 photoelectrons and

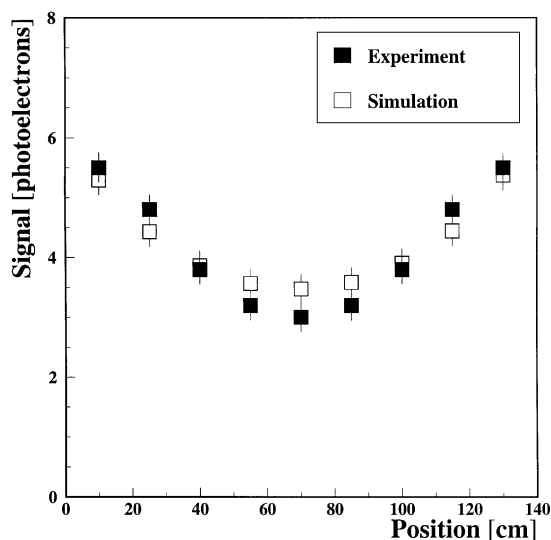


Fig. 2. Simulated and experimental numbers for the prototype SKS Cherenkov as functions of the detector's width.

a multiplicity of 4. The simulated and experimental uniformity were also in agreement. No experimental timing data are available. Also, a detailed comparison is made with the very wide prototype SKS detector [11] and is shown in Fig. 2.

The first detector designed using the simulation program was the large, $210 \times 50 \times 24$ cm³, NIKHEF BigBite Cherenkov detector [12]. The program predicted that the detector would produce an average signal of 7.2 photoelectrons and have a timing FWHM of 3.4 ns. During commissioning,² the detector produced an average signal of 6.8 photoelectrons and had a timing FWHM of 3.6 ns. The uniformity curves are shown in Figs. 3 and 4. In both the simulated and experimental plots, the peaks correspond to the location of the photomultiplier tubes along the sides of the detector. The plots are shown for the same number of events and have not been scaled. No experimental multiplicity data are available.

Recently, the simulation code was used to design the aerogel Cherenkov detectors for the Bates

²In the 1.5 years since commissioning, the detector's signal has degraded to 6.1 ± 0.5 photoelectrons.

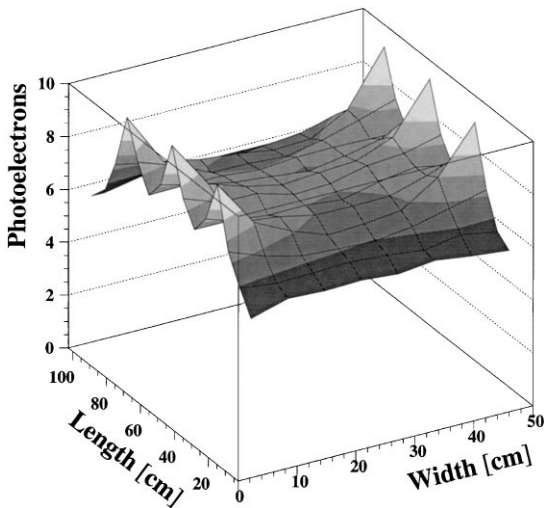


Fig. 3. The predicted signal uniformity of the BigBite Cherenkov detector is shown. The six peaks correspond to the locations of photomultiplier tubes along the sides of the detector.

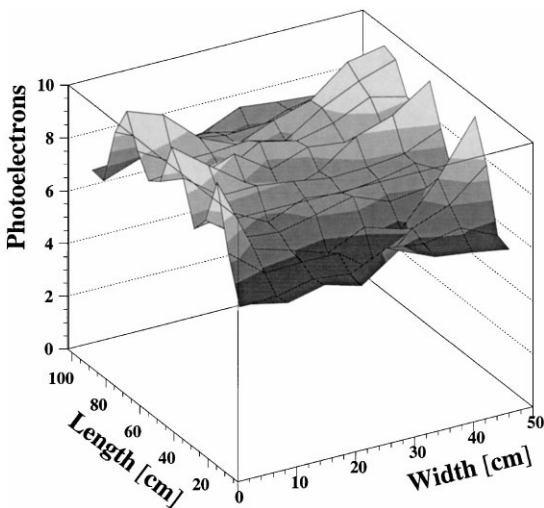


Fig. 4. The actual signal uniformity of the BigBite Cherenkov detector is shown. As predicted, the six peaks due to the location of the photomultiplier tubes can be clearly identified. The location of electron events passing through the detector were determined using two wire chambers located immediately in front of the detector.

Large Acceptance Spectrometer Toroid, BLAST [13]. These Cherenkovs will be $100 \times 150 \times 30 \text{ cm}^3$ and filled with 15 cm of aerogel with a refractive index of 1.03. The detector should produce an

average signal of around 4.5 photoelectrons and have an average efficiency of 99%. The code has also been used to consider the feasibility of adding a Cherenkov detector to the Bates OOPS spectrometers [14] and to simulate Cherenkov detectors for TJNAF [15].

4. Figure of merit values

The figures of merit, H , for the detectors listed in Table 1 are shown in Fig. 5. The results show that the H value for a typical large aerogel Cherenkov detector lies within a region bounded by the solid lines drawn on the graph. The bounding lines have slopes of -1.56 and -1.10 cm^{-2} and H intercepts of 48 and 33 cm^{-1} .

Though only one point is shown below the lower line, private communications with P.J. Carlson and G. Poelz revealed that many unpublished first attempts at Cherenkov construction have H values in the poor region. The primary reason for poor results is aerogel contamination. Aerogel which has been contaminated can be baked out, as has been

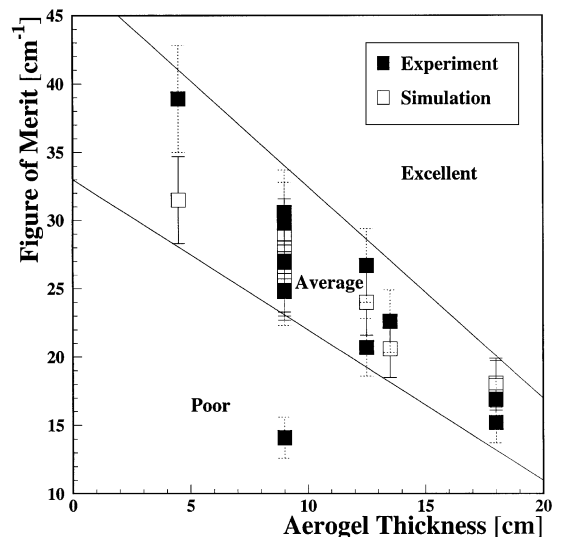


Fig. 5. Shown are simulated and experimental figures of merit, H , from Table 1. The graph has been broken into three regions: poor, average, and excellent. The point in the poor region corresponds to a detector which contained contaminated aerogel.

demonstrated with the excellent second result of the CEBAF Cherenkov detector, as shown in Table 1.

By using the range of values shown in Fig. 5, a designer can use the phenomenological equation to predict the signal strength of a planned detector. The phenomenological equation should be used with caution when being used for a detector wider than 50 cm, 25 cm for Cherenkov detectors with photomultipliers on only one side. Though the equation will still provide good information about average signal strength, wide detectors will not necessarily produce a uniform signal and should be simulated. This was shown with the 140 cm wide prototype SKS Cherenkov detector in Fig. 2. In order for this exceptionally large detector to produce a uniform signal, special reflectors were added to the middle of the light box region.

5. New aerogel

Improvements in the way aerogel is manufactured has led recently to the development of silica aerogel with extremely long absorption lengths [16,17]. It has been found that these new aerogels have absorption lengths 100 times their scattering length [18]. Thus, for high transparency aerogel, the absorption length in Eq. (5) can be replaced by 1000 cm.

To check the validity of the simulation program with this new parameter, the Cherenkov detector of the BELLE detector [18] was simulated. In order to simulate a detector with this new aerogel, it was assumed that once the Cherenkov radiation had been produced, the aerogel could be ignored. Thus the entire interior of the Cherenkov detector was considered to be the light box region of the detector and all walls were taken to have an average of 96% reflectivity. The results of the experiment and simulation are shown in Fig. 6.

To show the improvement that the new aerogel can produce, the detectors listed in Table 1 have been simulated with the new aerogel. The results are shown in Fig. 7. With the long attenuation length aerogel, the figure of merit has a relatively constant value for different thicknesses of aerogel.

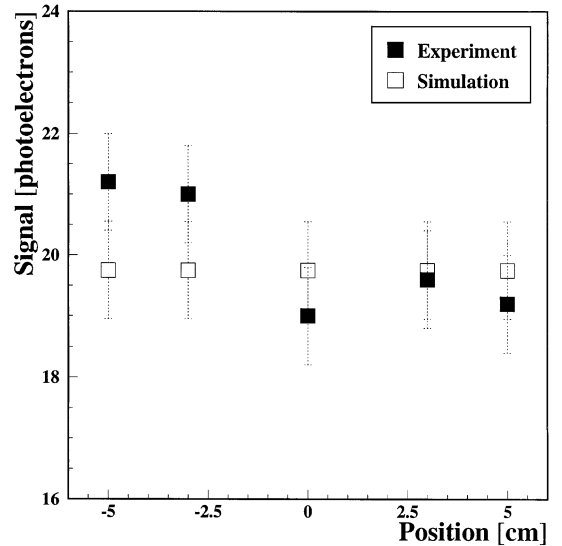


Fig. 6. Simulation comparison with the BELLE Cherenkov which contains the new, long attenuation length aerogel. The figure is plotted for the BELLE 4 cm y-position.

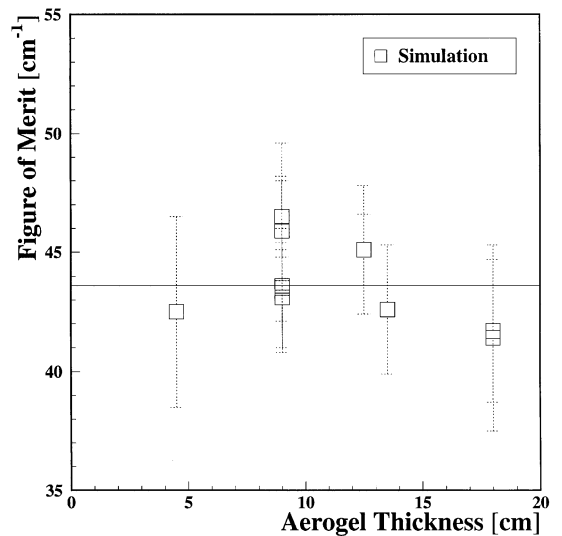


Fig. 7. Simulation results showing the figure of merit, H_{new} , versus aerogel thickness for the new aerogel.

Therefore, Eq. (7) can now be written

$$N_c = H_{\text{new}} L (1 - 1/\beta^2 n^2) \frac{\varepsilon}{1 - \eta(1 - \varepsilon)}, \quad (10)$$

where $H_{\text{new}} = 43.5 \text{ cm}^{-1}$.

The new aerogel is being considered [19] for the Blast Cherenkov detectors mentioned in Section 3. The new aerogel would allow the detector to be built to the same signal and uniformity specifications while using only one third as much aerogel. Currently, the only major drawback to this new, high transparency aerogel is its cost.

6. Detector lifetime

All the aforementioned results yield the number of photoelectrons a diffusely reflective Cherenkov detector will produce when the detector is new. It is important to realize that even a carefully constructed detector's signal will degrade over time. This is mainly due to contaminants being absorbed by the aerogel causing the absorption length to decrease and/or the diffusely reflective surfaces aging and becoming less reflective. Though few published works chart detector signal versus time, those results that are available [4,10] and the BigBite detector result, suggest that a typical signal half-life is approximately 10 years.

7. Summary and conclusions

The phenomenological equation, along with the figure of merit curves, will allow designers to calculate quickly the expected photoelectron values for a given Cherenkov design. For detectors that are too wide to reliably use the phenomenological equation or when more precise prediction is required, the simulation program can be used to ensure that a detector will not only produce a sufficient photoelectron signal, but also will produce a uniform signal, have good timing characteristics, and have a sufficient multiplicity.

Since these simulation techniques use nominal values for many unknowns, the results should only be used to determine what the nominal results of

a given detector should be. The results should not be taken as an exact representation of any one detector, but if a detector fails to produce even a nominal result, it should suggest that there is a problem with the detector, such as aerogel contamination.

Acknowledgements

I would like to thank H. Breuer, B.E. Norum, J. Steijger, and M.L. Stutzman for their help and advice in preparing this work. This research was supported by DOE grant DE-FG05-87ER40364.

References

- [1] S. Henning et al., *Phys. Scripta* 23 (1980) 703.
- [2] G. Poelz, *Nucl. Instr. and Meth. A* 248 (1986) 118.
- [3] H. Burkhardt et al., *Nucl. Instr. and Meth.* 184 (1981) 319.
- [4] P.J. Carlson et al., *Nucl. Instr. and Meth.* 160 (1979) 407.
- [5] J.D. Jackson, *Classical Electrodynamics*, 2nd ed., Wiley, New York, 1975.
- [6] M. Cantin et al., *Nucl. Instr. and Meth.* 118 (1974) 177.
- [7] P. Carlson, *Nucl. Instr. and Meth. A* 248 (1986) 110.
- [8] M. Benot et al., *Nucl. Instr. and Meth.* 154 (1978) 253.
- [9] H. Breuer, private communication.
- [10] H. Castricum, Commissioning of detectors for experiments at NIKHEF, Master's Thesis, University of Amsterdam, 1995.
- [11] T. Hasegawa et al., *Nucl. Instr. and Meth. A* 342 (1994) 383.
- [12] D.J. de Lange et al., *Nucl. Instr. and Meth. A* 406 (1998) 182.
- [13] R. Alarcon et al., Blast technical design report, Technical Report, Bates Linear Accelerator Center, 1997.
- [14] Z.L. Zhou, private communication.
- [15] C.W. de Jager, B. Wojtsekhowski, private communication.
- [16] K. Arisaka et al., *Nucl. Instr. and Meth. A* 379 (1996) 460.
- [17] A. Buzykaev, *Nucl. Instr. and Meth. A* 379 (1996) 465.
- [18] R. Suda et al., *Nucl. Instr. and Meth. A* 406 (1998) 213.
- [19] R. Alarcon, private communication.
- [20] P. Dunn, *Nucl. Instr. and Meth.* 224 (1984) 106.
- [21] C. Arnault et al., *Nucl. Instr. and Meth.* 177 (1980) 337.
- [22] P.J. Carlson, M. Poulet, *Nucl. Instr. and Meth.* 166 (1979) 425.